

## Investigation on the effect of spinning conditions on the properties of hollow fiber membrane for hemodialysis application

Sumarni Mansur,<sup>1</sup> Mohd Hafiz Dzarfan Othman,<sup>1</sup> A. F. Ismail,<sup>1</sup> Siti Hamimah Sheikh Abdul Kadir,<sup>2</sup> Fatmawati Kamal,<sup>2</sup> Pei Sean Goh,<sup>1</sup> Hasrinah Hasbullah,<sup>1</sup> Bee Cheer Ng,<sup>1</sup> Mohd Sohaimi Abdullah<sup>1</sup>

<sup>1</sup>Advanced Membrane Technology Research Centre (AMTEC), Faculty of Chemical and Energy Engineering (FCEE), Universiti Teknologi Malaysia, 81310 UTM, Skudai, Johor, Malaysia

<sup>2</sup>Institute of Molecular Medicine and Biotechnology, Faculty of Medicine, Universiti Teknologi Mara Sungai Buloh Campus, Jalan Hospital, Sungai Buloh, Selangor, 47000, Malaysia

Correspondence to: M. H. D. Othman (E-mail: hafiz@petroleum.utm.my)

**ABSTRACT:** Polyethersulfone (PES) hollow fiber membranes were fabricated via the dry-wet phase inversion spinning technique, aiming to produce an asymmetric, micro porous ultrafiltration hollow-fiber specifically for hemodialysis membrane. The objective of this study is to investigate the effect of spinning conditions on the morphological and permeation properties of the fabricated membrane. Among the parameters that were studied in this work are air gap distance, dope extrusion rate, bore fluid flow rate, and the take-up speed. The contact angle was measured to determine the hydrophilicity of the fibers. Membrane with sufficient hydrophilicity properties is desired for hemodialysis application to avoid fouling and increase its biocompatibility. The influences of the hollow fiber's morphology (i.e., diameter and wall thickness) on the performance of the membranes were evaluated by pure water flux and BSA rejection. The experimental results showed that the dope extrusion rate to bore fluid flow rate ratio should be maintained at 1:1 ratio to produce a perfectly rounded asymmetric hollow fiber membrane. Moreover, the flux of the hollow fiber spun at higher air gap distance had better flux than the one spun at lower air gap distance. Furthermore, spinning asymmetric hollow fiber membranes at high air gap distance helps to produce a thin and porous skin layer, leading to a better flux but a relatively low percentage of rejection for BSA separation. Findings from this study would serve as primary data which will be a useful guide for fabricating a high performance hemodialysis hollow fiber membrane. © 2016 Wiley Periodicals, Inc. *J. Appl. Polym. Sci.* **2016**, *133*, 43633.

**KEYWORDS:** hydrophilic polymers; membranes; morphology; properties and characterization

Received 30 September 2015; accepted 11 March 2016

DOI: 10.1002/app.43633

### INTRODUCTION

In recent years, there has been a crucial rise of kidney failure notably chronic kidney disease (CKD) caused by a disease or condition that impairs kidney function, causing kidney damage to worsen over several months or years as reported by National Kidney Foundation Malaysia (2012). Hemodialysis is one of the prominent treatment for CKD. This procedure helps to filtrate water, waste product and uremic toxins from the blood and to balance the pH value in the body. During hemodialysis, blood removed from the body is delivered to a hemodialyzer (artificial kidney). Inside the hemodialyzer, blood flows through a dialysis membrane, which contains pores large enough to permit the diffusion of small solutes. Smaller size of uremic toxins such as urea and creatinine are able to pass through the semipermeable membrane with ease. Barzin *et al.*<sup>1</sup> stated that uremic toxins such as urea and creatinine, ranging from size 10 to 55 kDa, needs to be excreted out from the blood. While, proteins such

as albumin (66 kDa) need to be retained. However, middle molecule such as  $\beta_2$ -microglobulin has a low diffusion clearance due to bounding of uremic toxins to larger size of protein. This problem can be solved by using a high flux semipermeable membrane.<sup>2-4</sup> The higher pore size allows the penetration of this protein bound molecule and at the same time retains larger molecule such as albumin.

In hemodialysis, two principles of solute removal are applied, which are diffusion and convection. Diffusion is the primary principle of solute transport in hemodialysis where small enough solutes passing through the semipermeable dialysis membrane are being diffused out down a concentration gradient. Convection, on the other hand, is the solute clearance during hemofiltration where solute and fluid is removed across semipermeable membrane down a pressure gradient (solvent drag). In this process, fluid flux is necessary for the removal of solutes during hemofiltration. Thus, it is vital to determine the

value of the fluid flux of the membrane. Flux relates to the ultrafiltration coefficient (Kuf) of the membrane, the rate at which water crosses the membrane at a given transmembrane pressure.<sup>5</sup> According to Food and Drug Administration (FDA), the *in vitro* Kuf for a conventional hemodialyser would be equal to or less than 12 mL/h/mmHg or beta-2 microglobulin clearance less than 10 mL/min. Whereas, the high-flux hemodialyser would be higher than 12 mL/h/mmHg or beta-2 microglobulin clearance greater than 20 mL/min.<sup>6,7</sup>

For hemodialysis ultrafiltration hollow fiber membrane application, the membrane produced is preferred to be high flux, asymmetric, thin micro porous ultrafiltration hollow fiber membrane.<sup>8–10</sup> Thin membrane is able to increase the amount of permeate produced.<sup>11</sup> However, to produce such desired membrane, the hollow fiber does not only need to be thin but also has to be extra small in diameter as compared to other ultrafiltration membrane. Small and thin membranes will increase the surface area of the membrane which will allow more blood to be exposed to dialysate. Consequently, more solutes can be removed from the blood. Common haemodialyzer surface area can range from 0.5 to 2.4 m<sup>2</sup>.<sup>10</sup> For a common ultrafiltration membrane, the internal diameter (ID) of the hollow fiber ranges from 0.6 to 1.1 mm. From the study conducted by Hayama *et al.*,<sup>12</sup> the commercially hollow fiber membrane of APS-150 (Asahi-medical, Japan) has an ID of 210 μm and a wall thickness of 45 μm.

PVP is the common and widely used hydrophilic polymer additive to enhance the PES membrane properties, especially in hemodialysis application. The addition of the PVP increases the solvent-water exchange during phase inversion stage. In addition, PVP is also a water soluble pore forming agent/polymer which increases the membrane porosity and finger-like void.<sup>12</sup> Though most of the PVP polymer leaks out during the phase inversion stage, some of the PVP remain in the fibers and will increase the hydrophilicity of the membrane. Thus, the passage of water through the membrane will be increased. This could result in better removal of uremic toxins that are water soluble through the semi-permeable membrane.<sup>13</sup>

PES hollow fiber membrane has been used in several of medical field application including tissue culture media sterilization, life science and microbiology fluid applications, clinical, and general filtration. Manufacturers often choose PES membranes for applications requiring high-flux, low-to-moderate protein binding, and high resistance to chemical cleaning and sanitization solutions. The fact that PES comes with astonishing characteristics such as outstanding oxidative, thermal, and hydrolytic stability as well as good mechanical property makes PES polymer widely employed in biomedical fields such as artificial organs and medical devices used for blood purification such as hemodialysis. Hence, PES hollow fiber membranes was a good candidate for manufacturing hemodialyser. Furthermore, there are few studies that have proved the biocompatibility of PES membrane in contact with blood.<sup>14–16</sup> Thus, PES polymer is used in this study due to its effectiveness and biocompatibility as a dialysis membrane.

Many research work done on the characterization of the hemodialysis hollow fiber membrane were focused on the chemical compositions and biocompatibility of the polymer. There are also

few studies discussed on the distribution of the pore size during fabrication of hemodialysis membrane.<sup>17,18</sup> However, lesser amount of studies was done on the spinning parameters for hemodialysis membrane, in which most of these studies were specifically for water treatment application. Therefore, in this study, the effect of spinning parameters of phase inversion technique on the morphology and permeation property of hemodialysis hollow fiber membrane was investigated. This may lead to a new finding that could possibly be a basis for the next move in fabricating high performance hemodialysis membrane. Positive result can benefit to the membrane field of research especially in membrane technology for hemodialysis application.

## EXPERIMENTAL

### Materials

Polyethersulfone (PES, Veradel<sup>®</sup> A-301) was purchased from Solvay Advanced Polymers (USA). Poly(vinyl pyrrolidone) (PVP, K25) was purchased from Sigma-aldrich (Germany). *N,N*-Dimethylacetamide (DMAc; AR, 98%) and bovine serum albumin (BSA) ( $M_w = 67,000$ ) were supplied by Quality reagent chemical (New Zealand) and Sigma (USA), respectively.

### Membrane Fabrication

PES pellet was dried in oven at 50 °C for 24 h to remove moisture content prior to dope solution preparation. Polymeric dope solution comprising of 18 wt % PES, 3 wt % PVP, and 79 wt % DMAc was prepared. PVP was used as the pore forming agent. The viscosity of the dope solution was measured by Cole-Parmer<sup>®</sup> viscometer. The dry-wet spinning technique was used for the preparation of hollow fibers as shown in Figure 1. In this formation process of a membrane, two types of phase inversion can be distinguished. The dry phase inversion takes place in the atmosphere by evaporation of the volatile solvent. While, the wet phase inversion is carried out by immersing the polymer solution membrane into a coagulation bath of a non-solvent where the membrane was formed.

The outer and inner diameters of the spinneret were 0.6 mm and 0.3 mm, respectively, and the bore fluid and coagulation bath composition used throughout the experiment were distilled water and normal tap water respectively. The extrusion ratio was calculated according to the following equation:

$$\text{Extrusion ratio, } R = \frac{A_0}{A_f} \quad (1)$$

Where  $A_0$  is the initial cross-sectional area of the spinneret and,  $A_f$  is the final cross-sectional area of the spinneret. The extrusion ratio helps in determining the dope extrusion rate and bore fluid flow rate that was used in the study on the effect of air gap on the hollow fiber membrane.

The dope solution and bore fluid were extruded through the spinneret to form the hollow fiber at the ambient temperature. The nascent hollow fiber was passed through certain air gap distance before entering into coagulation bath at room temperature. The hollow fiber was passed through two coagulation baths and collected at collection drum. The 1st coagulation bath will have a higher concentration of solvent after a period of dope extrusion due to accumulation of solvent extruded from the fiber. However, 2nd coagulation bath helps to maintain the fiber

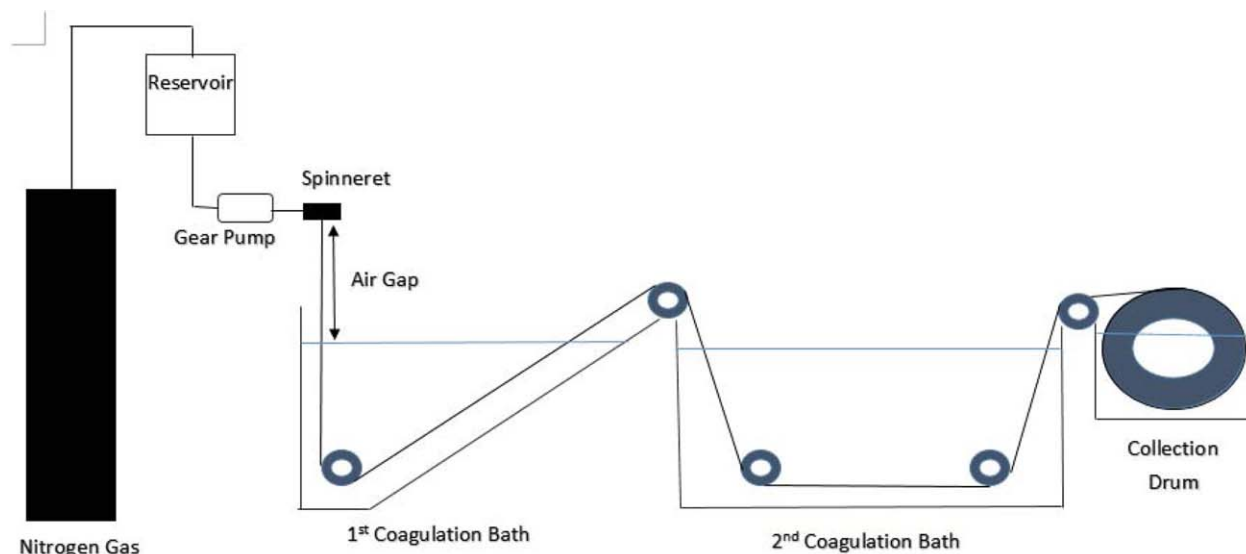


**Figure 1.** Schematic diagram of dry/wet inversion spinning technique. [Color figure can be viewed in the online issue, which is available at [wileyonlinelibrary.com](http://wileyonlinelibrary.com).]

passing through fresh water and improves the solidification of the fiber reaching at collection drum for collection. The air gap length, dope extrusion rate (DER), and bore fluid flow rate (BFFR) were manipulated and controlled throughout the experiment. Furthermore, the PES/PVP dope solution viscosity was 381.3 mPa s.

The spinning parameters for different air gap distance and different dope extrusion rate and bore fluid flow rate are shown in Table I.

#### Contact Angle Measurement

The contact angle measurement was measured by contact angle system OCA (Dataphysics, USA). Static contact angles of the membrane surface were measured using the sessile drop method. A constant dosing volume of 0.2  $\mu\text{L}$  of pure water with 1.0  $\mu\text{L/s}$  of dosing rate was deposited with a micro syringe onto a dry membrane in air and the contact angle was recorded. The average of 10 measurement for each fibers contact angle was recorded.

#### ATR-FTIR

ATR-FTIR spectra was recorded on a Thermo spectrometer (Nicolet 5700 FTIR). FTIR results can display the change of the functional groups and elemental in the polymers, and can characterize covalent bonding information. FTIR analysis is applied

to the hollow fiber membrane to ensure the existence of the PVP incorporated in the membrane after the blending and membrane fabrication procedure.

#### Adsorption/Desorption Experiment

Adsorption/desorption measurement was performed with a Micromeritics AutoChem II 2920 (Micromeritics, USA) analyser to determine of the surface area and porosity of the fiber spun at different air gaps. All fibers were degassed by being heated at 140  $^{\circ}\text{C}$  for 12 h, prior to the adsorption experiments. The BET (Brunauer–Emmet–Teller) surface area was obtained by applying the BET equation. The pore volume and pore size were obtained by  $p/p^0 = 0.95$  to the adsorption data and BJH (Barrett–Joyner–Halenda) method, respectively.

#### Pure Water Flux

The pure water permeation flux of the hollow fiber membranes was measured by ultrafiltration experiment system. The pure water flux was calculated from the eq. (2),

$$\text{Flux (L/m}^2 \cdot \text{h)} = \frac{V}{At} \quad (2)$$

where  $V$  is the volume of permeation (L),  $A$  is the total area of the hollow fibers ( $A$ ), and  $t$  is the time taken (h).

**Table I.** Spinning Parameters for Different Air Gap Distance, Different Dope Extrusion Rate (DER), Bore Fluid Flow Rate (BFFR), and Speed during Membrane Collection (CD)

Sample	Air gap (cm)	DER (cm <sup>3</sup> /min)	BFFR (cm <sup>3</sup> /min)	CD (Hz)	Sample	Air gap (cm)	DER (cm <sup>3</sup> /min)	BFFR (cm <sup>3</sup> /min)	CD (Hz)
A-1-1	3	3	1	4.5	A-2-1	50	1	1	5.0
A-1-2	10	3	1	4.5	A-2-2	50	2	2	8.0
A-1-3	25	3	1	5.0	A-2-3	50	3	2	10.0
A-1-4	50	3	1	7.3	A-2-4	50	4	1.33	12.0
A-1-5	75	3	1	10.0	A-2-5	50	5	1.67	14.0
A-1-6	100	3	1	11.5	A-2-6	50	1	0.33	4.0

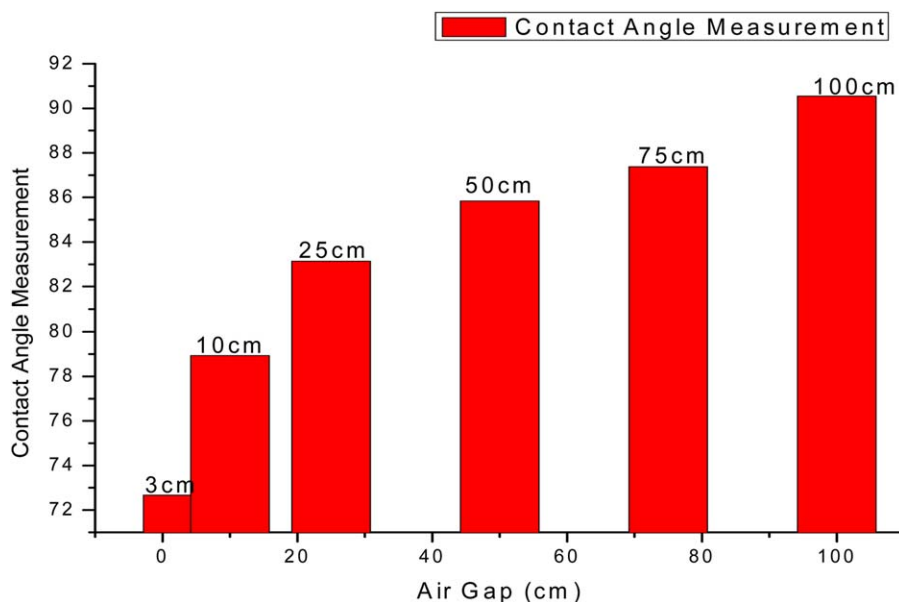


**Figure 2.** Contact angle measurement for hollow fiber spun with different air gap between spinneret and coagulation bath and constant DER ( $3 \text{ cm}^3/\text{min}$ ) and BFFR ( $1 \text{ cm}^3/\text{min}$ ). [Color figure can be viewed in the online issue, which is available at [wileyonlinelibrary.com](http://wileyonlinelibrary.com).]

For pure water flux experiment, tap water was used as the feed and the system was allowed to run for first 10 min to stabilize the pressure and to ensure water completely filling in the module. For every 10 min the permeation was collected and measured. The pure water flux and permeability testing were repeated three times for each sample to get a reliable value.

The permeability of the membrane was calculated from the eq. (3),

$$\text{Permeability} = \frac{\text{flux}}{\text{pressure}} \quad (3)$$

#### Rejection of Bovine Serum Albumin (BSA)

The rejection of BSA was measured using the same ultrafiltration experiment system. All modules were run under a pressure of 0.5 bar and 10 mL of the permeation was collected. 500 ppm BSA (67,000 Da) solution was used in membrane rejection testing. The infiltration and feed were determined by a UV-spectrophotometer (DR-5000TM, Canada). The test was repeated three times for each sample to get a reliable value. The rejection (R) was obtained by the formula (3),

$$R = \left[ 1 - \frac{C_P}{C_F} \right] \times 100\% \quad (3)$$

where R is the rejection to BSA (%) and,  $C_P$  and  $C_F$  are permeate and feed concentrations, respectively (wt %).

#### Scanning Electron Microscopy

The hollow fiber membrane samples' morphological studies were viewed on TM3000 Tabletop scanning electron microscope (Hitachi, USA) under magnifications ranging from 100x to 10,000x. For hollow fiber cross section sample preparation, the hollow fiber was immersed and snapped under liquid nitrogen in order to produce a clean-cut surface. Next, all samples were sputtered with gold by using an ion-sputtering SC7620 sputter coater (Quorum Technologies, UK).

#### AFM Observation

The AFM studies were conducted using a Park XE-100 AFM (Park Systems, CA). The membrane surface morphology was expressed in terms of mean surface roughness ( $R_a$ ). The mean surface roughness is the mean value of the surface relative to the center plane, the plane for which the volumes were enclosed by the equal number of images above and below this plane. The roughness parameters are dependable on the treatment of the captured surface data (plane fitting, flattening, filtering, etc.).

## RESULTS AND DISCUSSION

#### Characterization of Membrane Spun at Different Air Gap

The water contact angle is used to evaluate the hydrophilicity of the membrane. The air gap and DER affect the composition of

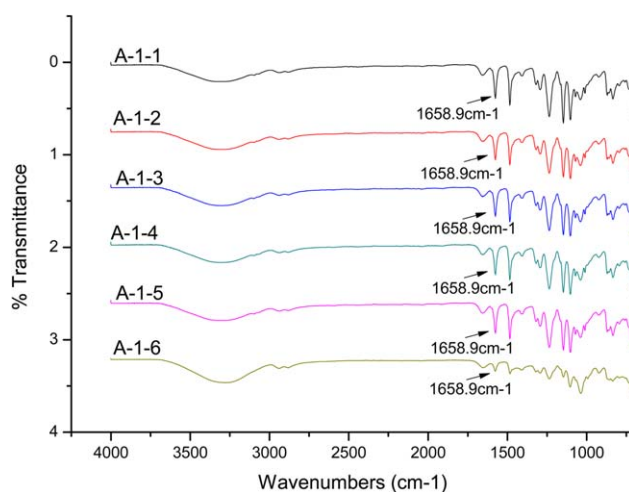


**Figure 3.** ATR-FTIR analysis for hollow fiber spun with different air gap between spinneret and coagulation bath and constant DER ( $3 \text{ cm}^3/\text{min}$ ) and BFFR ( $1 \text{ cm}^3/\text{min}$ ). [Color figure can be viewed in the online issue, which is available at [wileyonlinelibrary.com](http://wileyonlinelibrary.com).]

**Table II.** Physical Properties of the Membranes Spun at Different Air Gap Distance

Sample	BET surface area (m <sup>2</sup> /g)	Volume of mesopore (cm <sup>3</sup> /g)	BJH pore size (nm)	Porosity (%)
A-1-1	16.25946	0.0347	34.32409	64.03
A-1-2	15.47390	0.0356	33.35876	64.24
A-1-3	15.08347	0.0346	33.32678	65.65
A-1-4	14.47419	0.0345	32.27339	66.21
A-1-5	13.89372	0.0337	31.35246	66.48
A-1-6	13.00382	0.0330	31.01435	67.78

the hollow fiber membrane produced. Although the composition (PES/PVP/DMAc) and the dope viscosity for all the fibers are the same, the hydrophilicity of the membrane increase with the increase of air gap distance. Addition of PVP polymer is proposed to chemically modify the polymer to increase the hydrophilicity of PES membranes. From the result in Figure 2, it is assumed that during the phase inversion, the PVP may have been escaped into the bore fluid along the air gap distance due to its hydrophilic characteristic. The higher the air gap, the longer time was needed for the contact between bore fluid and PVP. Thus, more PVP leach out from the membrane and less PVP remain in the fibers, which explains that the membrane spun at a lower air gap distance is more hydrophilic compared to the membrane spun at a higher air gap distance.

The presence of PVP in the PES hollow fiber membrane was confirmed by the ATR-FTIR spectrum as shown in Figure 3. It should be pointed out that the characteristic peaking at 1658.9 cm<sup>-1</sup> was an overlapped peak for the C=O stretching in the -PVP chain and the -PES chain. Compared with the peaks at 1658.9 cm<sup>-1</sup> for the hollow fiber membrane spun at different air gaps, it was observed that the peaks of the lower air gap were stronger than that of the higher air gap, which indicated that there were abundant block copolymers on the membrane spun at lower air gap distance compared to higher air gap distance.

As mentioned in the introduction, hemodialysis was applied on two principles of solute removal which is diffusion/dialysis and convection/ultrafiltration. A hollow fiber membrane permeability is based on the sizes and number of pores that allow the solution or solute to enter and pass through the other side.<sup>19</sup> Hemodialysis application typically uses membrane material with mesopore and ultramicropore, which is suitable for ultrafiltra-

tion and dialysis application, respectively. Variations in the pore size distribution and porosity may result in differences in both permeability and solute rejection for the membrane.<sup>19</sup>

Table II shows the physical properties of the fibers. The hollow fiber membrane produced membrane with mesopore which is suitable for ultrafiltration application (good in solute removal). It can also be seen that the values of BET surface area, volume of mesopore and BJH pores sizes of fibers spun at different air gap distance are very close. As air gap distance increases, the BET surface area, volume of mesopore and BJH pores size also increase. The porosity for the fibers shows a percentage up to 60%. Low porosity will result in low permeability which explains the low permeability of the membrane as shown in Table III.

#### Pure Water Flux and BSA Rejection

The membrane performance was evaluated by pure water flux and percentage of solutes rejection. The fluid flux is necessary for solute removal during hemofiltration. In this study, water is used as the preliminary studied to determine the membrane performance in term of permeability. The normal range of protein to be retained during hemodialysis range from size 64 to 66 kDa. Thus, Bovine serum albumin (BSA) with molecular weight of 67 kDa was used as the marker to determine the percentage of solutes rejection. Higher percentage value of solutes rejection means that the membrane able to retain more protein. The results of ultrafiltration experiments and protein rejection are summarized in Table III. Although the hollow fiber possesses high protein rejection, which is more than 80% of BSA rejection, some of the hollow fibers have poor pure water flux permeation results. This is the common trade off phenomena in membrane fabrication and these results correlates with the morphology of the membranes produced. Based on Table III, hollow

**Table III.** Water Permeability and Protein Rejection of the Hollow Fiber Membrane

Sample	Air gap (cm)	Permeability (ml/cm <sup>2</sup> min/mmHg)	BSA rejection (%)
A-1-1	3	1.79 × 10 <sup>-5</sup>	100
A-1-2	10	3.47 × 10 <sup>-5</sup>	91
A-1-3	25	5.49 × 10 <sup>-5</sup>	89
A-1-4	50	3.56 × 10 <sup>-5</sup>	93
A-1-5	75	6.99 × 10 <sup>-5</sup>	89
A-1-6	100	3.73 × 10 <sup>-5</sup>	97

**Table IV.** The OD and ID of the Membrane with Different Air Gap Lengths

Sample	Air gap (cm)	OD (μm)	ID (μm)	Resident time (s)
A-1-1	3	508	323	0.13
A-1-2	10	500	250	0.42
A-1-3	25	472	222	1.06
A-1-4	50	408	200	2.12
A-1-5	75	347	160	3.18
A-1-6	100	323	151	4.24

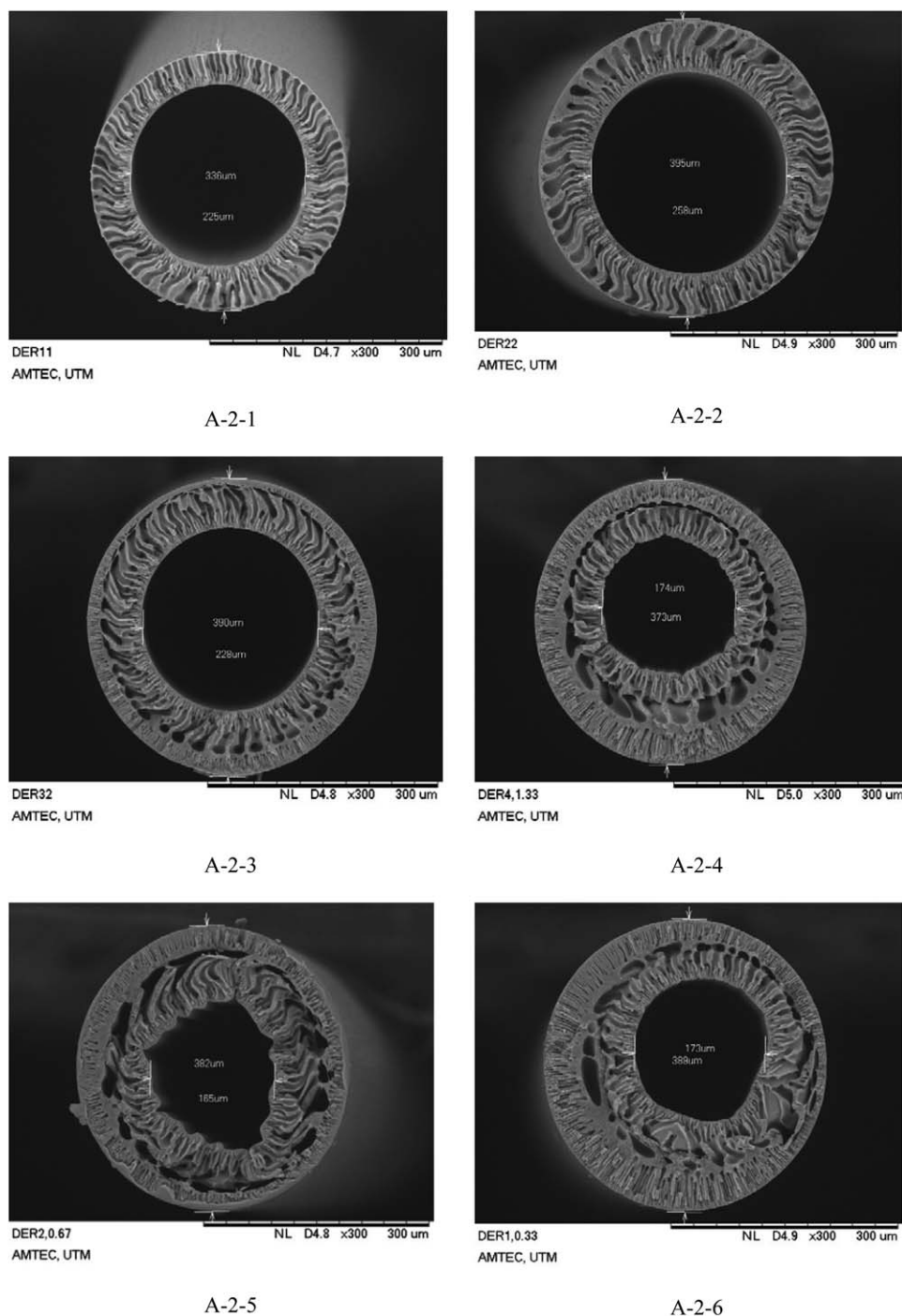


**Figure 4.** The SEM images of hollow fiber membrane with different dope extrusion rate (DER) and bore fluid flow rate (BFFR) spun at air gap 50 cm.

fiber membranes that were spun at 3 cm air gap shows the highest percentage of protein rejection which is 100% of protein rejection with the lowest reading of water permeability,  $1,79 \times 10^{-5}$  mL/cm<sup>2</sup> min/mmHg. This result can be explained based on the physical properties of the membranes in Table II, where the flux of the hollow fibers are influenced by porosity while the percentage protein rejection of the membranes are influenced by the pore size.<sup>20</sup> Hollow fiber membranes that were spun at 3 cm air gap produce higher pore size compared to others, resulting in high percentage of protein rejection but

at the same time have a low porosity which is causing a low water permeation. This result can also be related to with the contact angle measurement result of the membrane. The hydrophilic nature of the PVP reduces the membrane hydraulic resistance by increasing pores size and porosity of the membranes and consequently increases the pure water fluxes.<sup>21</sup>

#### Morphology

The outer diameter (OD) and inner diameter (ID) of the hollow fibers produced at different air gap lengths were measured

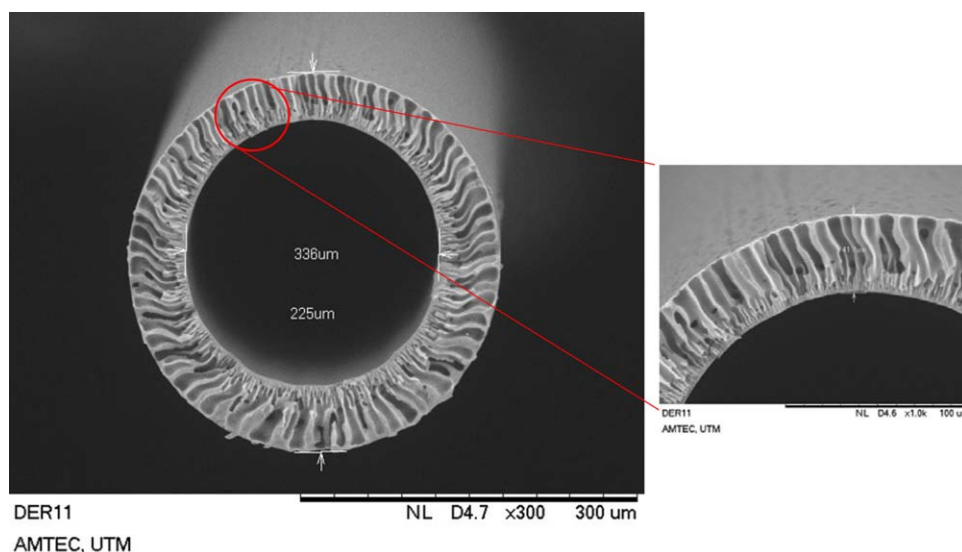


**Figure 5.** Cross sectional SEM pictures of sample A-2-1 hollow fiber membrane spun at 50 cm air gap region and DER and BFFR ratio of 1:1. [Color figure can be viewed in the online issue, which is available at [wileyonlinelibrary.com](http://wileyonlinelibrary.com).]

using SEM and were summarized in Table IV. Based on this data, it shows that the outer and inner diameters of the membrane decrease when the air gap between the spinneret and coagulation bath was increased. The resident time for the dope to be extruded and reached the coagulation bath increases when the air gap was increased, which indicates that more time for the elongational stresses of the nascent fiber, thus resulting to the smaller diameter of dried fiber. These results can be further explained based on elongational stresses in the air gap region connected to gravitational force or additional stretching during the take-up of fibers. High elongation stress will develop membrane porosity by pulling of the molecular chain apart in the early stage of phase separation.<sup>22</sup> Increasing the air gap will induced higher stretching of the nascent fiber due to the gravitational force.<sup>20,23,24</sup> When dope extrudes from the spinneret, it will swell and the elongation stress in the air gap region helps stretching the fiber. This resulted in elongation, higher spinning rate, and hence reduction of fiber dimensions.

Apparently, the size of the hollow fiber membrane is correlated with the performances of the hemodialysis membrane. Effectiveness of a haemodialyzer are determined by its clearance ( $K$ ) as shown in the formula (4).

$$KoA = \frac{Q_b Q_d}{Q_b - Q_d} \quad (4)$$

Clearance is expressed as the amount of blood (in mL) that is completely cleared of a certain solute in one minute of treatment, at a given blood flow rate ( $Q_b$ ) and dialysate flow rate ( $Q_d$ ).<sup>23</sup> The surface area ( $A$ ) is directly proportional to the clearance ( $K$ ), meanings that the higher the surface area of the membrane, the higher the clearance of the solute removal. This means that a smaller size of hollow fiber membrane could give a higher surface area, thus better performances in the clearance of the blood. The normal range of internal diameter of a synthetic haemodialyzer fibers ranges from 190  $\mu\text{m}$  to 240  $\mu\text{m}$  with outer diameter of 300  $\mu\text{m}$  to 400  $\mu\text{m}$  to have a urea clearance

of 250 mL/min at a  $Q_b$  of 300 mL.<sup>9</sup> This typical size of fibers can provide 1.0–2.5  $\text{m}^2$  of surface area.

Membrane that was spun at 50 cm air gap distance produced hollow fiber with internal diameter of 200  $\mu\text{m}$  which is the desired size of internal diameter for hemodialysis application. Furthermore, the membrane was spun at different air gap distances with constant DER, causing the membrane spun at higher air gap to be at the atmosphere at longer period as compared to the membrane spun at lower air gap. These facts could influence the formation of the internal surface of the membrane as humidity in the air gap may affect the inner surface during the formation of the membrane,<sup>25</sup> eventually causing the membrane to have unstable results as shown in Table III. Membrane spun at 50 cm air gap produces a suitable result for both permeability and solutes rejection. Thus, this air gap is used for further study in comparing the effect of different dope extrusion rates on membrane formation.

Apart from air gap distance, the dope extrusion rate to bore fluid flow rate ratio also plays a significant effect to the morphology of the hollow fiber membrane produced. From the SEM images in Figure 5, it can be seen that there is a ring-like structure produced in between the outer and inner surface of the fiber. These ring-like structure only exists with the fiber that is having a high ratio of dope extrusion rate to bore fluid flow rate during spinning process. This phenomena occurs due to the fact that there are delays in liquid-liquid demixing process at the fiber inner surface. Dope solution extrudes from the spinneret at a faster rate compared to the bore fluid flow rate, causing the polymer to have a lower concentration at its inner skin. When the outer skin had started to solidify, the inner skin was still in the process of precipitation and this caused bore fluid to be trapped in between outer and inner skin thus explaining the formation of the ring-like structure. Based on Figure 4, it can be suggested that the dope extrusion rate ratio to bore fluid flow rate should be maintained at 1:1 in order to obtain the desired perfectly rounded asymmetric, microporous ultrafiltration hollow fiber membrane.

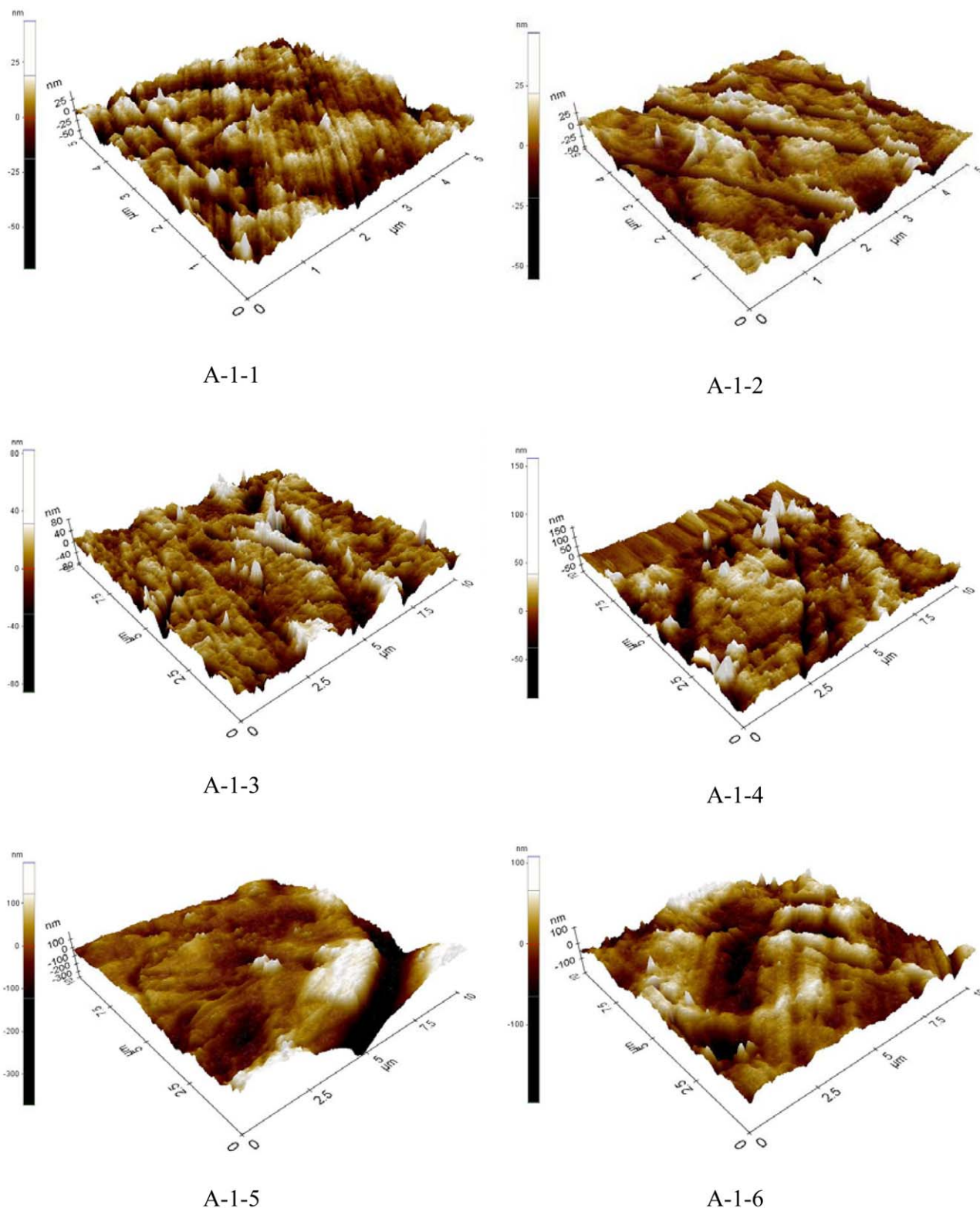


**Figure 6.** AFM images of hollow fiber membrane spun at different air gap distance. [Color figure can be viewed in the online issue, which is available at [wileyonlinelibrary.com](http://wileyonlinelibrary.com).]

Figure 5 shows the SEM images of the hollow fiber spun at 50cm air gap region with DER and BFFR ratio of 1:1, the cross sectional image shows a finger-like structure at the edge of the

membrane and becoming denser nearing the inner surface. Addition of PVP induced the pore forming during the phase inversion of the hollow fiber membrane, thus, producing a



**Table V.** Surface Roughness of the Hollow Fiber Membrane

Samples	$R_q$ (root mean square)	$R_a$ (mean surface roughness)	$R_z$ (different between high peak and lower valley)
A-1-1	9.639	7.579	108.230
A-1-2	16.730	12.181	162.181
A-1-3	23.001	18.127	162.367
A-1-4	15.544	10.689	190.233
A-1-5	29.726	22.423	253.715
A-1-6	48.020	36.039	396.153

highly asymmetric structure as shown in Figure 5. As a pore forming agent, PVP will leach out from the membrane during membrane fabrication, contributing to the formation of finger-like structure of the membrane. Asymmetric membrane consists of a very thin polymer layer on a highly porous thick sub-layer. The skin represents the selective layer of the membrane.

During hemodialysis, impure plasma that contains uremic toxic enter the lumen of the hollow fiber membrane and a cross-flow occurs between the plasma and dialysate. The dense area in the inner surface of the hollow fiber membrane as shown in Figure 5 is desired. This is because the inner membrane will be in direct contact with the blood which helps to filtrate the small uremic toxic out from the blood and enter the dialysate. The dense structure helps in retaining the desired protein-like red cell and albumin and releases of unwanted small molecules such as urea and creatinine from the blood and enter the dialysate. The finger-like structure near the end of the outer membrane will ease the movement of solutes from blood into the dialysate and will prevent any backflow of the solutes.

Figure 6 shows the 3D AFM images of the inner surface of the membrane spun at different air gap distances. The roughness parameters of these surfaces are shown in the Table V. On the basis of the result shown in Table V, it is seen that the roughness parameters of the membrane surfaces increase as the air gap distance increases.

## CONCLUSIONS

A suitable spinning parameters of dry-wet spun extra-small hemodialysis hollow fiber ultrafiltration has been studied. The air gap distances varied from 3 to 100 cm and spinneret of 0.6  $\mu\text{m}$  (outer diameter) and 0.3  $\mu\text{m}$  (inner diameter). Experimental results showed that the membrane spun at higher air gap distance had better flux than the membrane spun at lower air gap distance. The suitable membrane had a permeability of  $3.56 \times 10^{-5}$  and retention rate of 93% for BSA with outer and inner diameter of 408 and 200  $\mu\text{m}$ , respectively. This membrane was spun at 50 cm air gap distance. A desired of extra-small hollow fiber membrane was achieved with 408  $\mu\text{m}$  of outer diameter and 200  $\mu\text{m}$  of inner diameter.

## ACKNOWLEDGMENTS

The authors gratefully acknowledge financial support from Universiti Teknologi Malaysia under Flagship Program (Project number: Q.J130000.2409.01G46) and Ministry of Higher Education Malaysia under Fundamental Research Grant Scheme (Project Number: R.J130000.7809.4F282). The authors would also like to thank Research Management Centre, Universiti Teknologi Malaysia for the technical support.

## REFERENCES

- Barzin, J.; Madaeni, S. S.; Mirzadeh, H. *Iran. Polym. J.* **2005**, *14*, 353.
- Schrier, R. W. In *Atlas of Diseases of the Kidney*; Henrich, W. L.; Bennet, W. M., Eds.; Current Medicine: Philadelphia, **1999**; pp 1–6.
- El Arbagy, A. R.; Koura, M. A. E. A.; El Nasr, A. E. S. S. A.; Elbarbary, H. S. *Am. J. Clin. Med. Res.* **2014**, *2*, 36.
- Ambalavanan, S.; Rabetoy, G.; Cheung, A. K. High-Efficiency and High-Flux Hemodialysis; Current Medicine: Philadelphia, **1994**.
- Kerr, P. G.; Huang, L. L. *Nephrology* **2010**, *15*, 381.
- Guidance for the Content of Premarket Notifications for Conventional and High Permeability Hemodialyzers; U.S. Department of Health Services FDA, **1998**.
- Palmer, S. C.; Rabindranath, K. S.; Craig, J. C.; Roderick, P. J.; Locatelli, F.; Strippoli, G. F. M. *Cochrane Database of Systemic Review*, **2012**, 9.
- Krieter, D. H.; Hackl, A.; Rodriguez, A.; Chenine, L.; Moragues, H. L.; Lemke, H. D.; Wanner, C.; Canaud, B. *Nephrol. Dial. Transplant* **2010**, *25*, 212.
- Brouwer, D. J.; Carlson, W.; Coppinger, C.; Evan, K.; German, S.; Hansen, S.; Hlebovy, D.; Jonsson, D.; Ledebro, I.; Lleras, A.; Martinez, N.; Mikles, R.; Morales, M.; Neumann, M.; Rawls, F.; Ray, T.; Renal, K. R.; Shaw, T. C. *Core Curriculum for the Dialysis Technician: A Comprehensive Review of Hemodialysis*, 5th ed.; Medical Education Institute Inc.; Amgen Inc., **2012**.
- Curtis, J. *Dialysis Technology a Manual for Dialysis Technicians*; Delaney, K.; O'kane, P.; Roshto, B.; Sweeney, J., Eds.; Haemodialysis Devices, 4th ed.; Amgen Inc.: Thousand Oaks, CA, **2003**.
- Rugbani, A. Investigating the Influence of Fabrication Parameters on the Diameter and Mechanical Properties of Polysulfone Ultrafiltration Hollow-Fibre Membranes; MSc. Thesis, University of Stellenbosch, **2009**.
- Hayama, M.; Yamamoto, K.; Kohori, F.; Sakai, K. *J. Memb. Sci.* **2004**, *234*, 41.
- Barzin, J.; Madaeni, S. S.; Mirzadeh, H.; Mehrabzadeh, M. *J. Appl. Polym. Sci.* **2004**, *92*, 3804.
- Ma, L.; Su, B.; Cheng, C.; Yin, Z.; Qin, H.; Zhao, J.; Sun, S.; Zhao, C. *J. Memb. Sci.* **2014**, *47*, 90.
- Ran, F.; Nie, S.; Zhao, W.; Li, J.; Su, B.; Sun, S.; Zhao, C. *Acta Biomaterialia* **2011**, *7*, 3370.

16. Dahe, G. J.; Teotia, R. S.; Kadam, S. S.; Bellare, J. R. *Biomaterial* **2011**, *32*, 352.
17. Yang, Q.; Chung, T. S.; Santoso, Y. E. *J. Memb. Sci.* **2007**, *290*, 153.
18. Chung, T.; Xu, Z.; Lin, W. *J. Appl. Polym. Sci.* **1999**, *72*, 379.
19. Nath, K. *Membrane Separation Processes*; PHI Learning Pvt. Ltd. **2008**.
20. Widjojo, N.; Chung, T. S. *Ind. Eng. Chem. Res.* **2006**, *45*, 7618.
21. Khayet, M. *Chem. Eng. Sci.* **2003**, *58*, 3091.
22. Chung, T. S.; Hu, X. D. *J. Appl. Polym. Sci.* **1997**, *66*, 1067.
23. Ahmad, S. *Manual of Clinical Dialysis*; Scribner, B. H., Eds.; Springer: New York, **1999**, Vol. *40*, p 114.
24. Ali, A.; Awang, M.; Mat, R.; Johari, A.; Kamaruddin, M. J.; Sulaiman, W. R. W. *Adv. Mater. Res.* **2014**, *931932*, 168.
25. Chwojnowski, A.; Wojciechowski, C.; Dudziński, K.; Łukowska, E. *Biocybernetics Biomed. Eng.* **2009**, *29*, 47.